Phycological Research

Phycological Research 2016; **64:** 160–175 doi: 10.1111/pre.12133

Revisiting the 1991 algal bloom in shelf waters off Argentina: *Azadinium luciferelloides* sp. nov. (Amphidomataceae, Dinophyceae) as the causative species in a diverse community of other amphidomataceans

Urban Tillmann[1]* **and Rut Akselman**[2]

[1]Alfred Wegener Institute for Polar and Marine Research, Bremerhaven, Germany and [2]Instituto Nacional de Investigación y Desarrollo Pesquero-INIDEP, Mar del Plata, Argentina

SUMMARY

Species of the marine dinophycean genera *Azadinium* and *Amphidoma* (Amphidomataceae) mostly attract attention because of their production potential of the lipophilic polyether phycotoxin azaspiracid (AZA). The genus *Azadinium* probably has a very wide geographical distribution. Blooms of *Azadinium* from the continental shelf off Argentina have been observed back in the early 1990, but were just recently published, and the causative species, identified at that time as *Azadinium* cf. *spinosum*, could not unequivocally be determined. Here we retrospectively analyzed old archived samples of one of the South Atlantic *Azadinium* bloom from 1991 with electron microscopy. It turned out that the dominant nanoplanktonic dinophycean species in fact represent a new species which we describe here based on the morphology. *Azadinium luciferelloides* sp. nov. is a small (approximately 9–14 μm cell length) thecate dinoflagellate with the dominant plate pattern of the genus (Po, X, 4′, 3a, 6″, 6C, 5S, 6‴, 2⁗), and with a small antapical spine. *Azadinium luciferelloides* differed from all other described species of *Azadinium* by the position of the ventral pore, which was located on the right ventral side in a notch of an otherwise symmetric pore plate. In addition, we recorded and documented the presence of other similar sized species of the Amphidomataceae in the samples. Our finding of *Az. spinosum*, *Az. dalianense*, *Az. dexteroporum*, and *Amphidoma languida* are the first record for the South Atlantic and thus describe an important range extension of these species. The diversity and importance of the Amphidomataceae for South Atlantic spring bloom plankton is now known and taxonomically documented, but cultures and/or analysis of AZA in field samples of the area are needed to clarify the AZA production potential of the local species and populations in order to finally evaluate the risk potential of AZA for AZA shellfish contamination in the Southwestern Atlantic region.

Key words: Amphidomataceae, Argentina, *Azadinium*, *Azadinium luciferelloides*, new species.

INTRODUCTION

Amphidomataceae is a family of the Dinophyceae proposed by Sournia (1984) now encompassing the genera *Azadinium* and *Amphidoma* (Tillmann *et al.* 2012a), and to which there is a growing number of new described species and species transferred from other genera (Tillmann *et al.* 2014a). This taxonomic group attracted interest because some of its members have the capacity to synthesize azaspiracids (AZAs). These toxins caused a first incident of human poisoning and were chemically characterized in the 1990 decade (McMahon & Silke 1996; Satake *et al.* 1998), but a primary causative agent, *Azadinium spinosum* Elbrächter *et* Tillmann, was not identified before 2009 (Tillmann *et al.* 2009). Since then, other species of *Azadinium*, *Az. poporum* Tillmann *et* Elbrächter and *Az. dexteroporum* Percopo *et* Zingone, and *Amphidoma languida* Tillmann, Salas *et* Elbrächter have been shown to synthesize compounds of the AZA group (Krock *et al.* 2012; Percopo *et al.* 2013).

Azaspiracids are a group of lipophilic polyether toxins of more than 30 different analogues (Rehmann *et al.* 2008; Hess *et al.* 2014). In vivo and in vitro studies using mice and human cultured cell lines showed that it causes potent cytotoxic effects with a broad action spectrum (Twiner *et al.* 2012, 2014) and that it could cause teratogenesis in fish embryos (Colman *et al.* 2005). Symptoms of azaspiracid poisoning (AZP) in humans include diarrhea, stomach cramps, nausea and vomits after consumption of bivalve shellfish. Azaspiracid analogues have been detected in plankton hauls and have a widespread occurrence in the North Sea (James *et al.* 2003; Krock *et al.* 2009). Several species of bivalve mollusks including mussels, oysters, scallops and clams are known to accumulate AZAs (Furey *et al.* 2010; Salas *et al.* 2011). In addition, these compounds were also detected in a crab and a sponge from marine origin (Torgersen *et al.* 2008; Ueoka *et al.* 2009). Azaspiracids have been reported in shellfish from numerous geographical sites and seem to have a wide distribution which encompass the Atlantic coasts of various European countries including Denmark, France, Ireland, Norway, Portugal, Spain, Sweden and UK (James *et al.* 2002; Braña Magdalena *et al.* 2003; Amzil *et al.* 2008; Vale *et al.* 2008), the Atlantic coast of NW Africa (Taleb *et al.* 2006), United States (Trainer *et al.* 2013) and Canada (Mike Quilliam, pers. comm. in Twiner *et al.* 2008), China (Yao *et al.* 2010) and Japan (Ueoka *et al.* 2009) in the Asian Pacific;

*To whom correspondence should be addressed.
Email: urban.tillmann@awi.de
Communicating editor: Mitsunori Iwataki
Received 5 January 2016; accepted 1 April 2016.

and the Atlantic and Pacific coasts of South America in Brazil (Massucatto *et al.* 2014) and Chile (Álvarez *et al.* 2010; López-Rivera *et al.* 2010).

Taxa recognized as belonging to the Amphidomataceae by their morphological characteristics and phylogenetic affinities include the species of the genus *Azadinium*, i.e. *Az. spinosum*, *Az. obesum* Tillmann *et* Elbrächter, *Az. poporum*, *Az. polongum* Tillmann, *Az. dexteroporum*, *Az. dalianense* Luo Z., Gu H. *et* Tillmann, *Az. trinitatum* Tillmann *et* Nézan, *Az. cuneatum* Tillmann *et* Nézan, *Az. concinnum* Tillmann *et* Nézan, *Az. caudatum* (Halldal) Nézan *et* Chomérat var. *caudatum* and *Az. caudatum* var. *margalefii* (Rampi) Nézan *et* Chomérat (Tillmann *et al.* 2009, 2010, 2011, 2012b, 2014a; Nézan *et al.* 2012; Luo *et al.* 2013; Percopo *et al.* 2013). Furthermore, the family included species of the genus *Amphidoma*, for which nine species are described (Guiry 2015), but the most recently described *Amphidoma languida* (Tillmann *et al.* 2012a) is the only species of the genus for which phylogenetic and toxinological data are available. Geographic distribution of this clade appears to be wide and may increase to new areas as the analysis of the nanoplanktonic size fraction, to which most of these species belong, could progress. To our knowledge, *Azadinium* has been recorded in the North Sea, in sub-Arctic and central areas of the North Atlantic, in some localities of Atlantic European coasts, the Mediterranean Sea, the austral Southwest Atlantic, and in the eastern (China, Korea and New Zealand) and western (Mexico) Pacific (Akselman & Negri 2012; Hernández-Becerril *et al.* 2012; Nézan *et al.* 2012; Potvin *et al.* 2012; Gu *et al.* 2013; Percopo *et al.* 2013; Tillmann *et al.* 2014c; Kaufmann *et al.* 2015; Smith *et al.* 2016), as well as in the Black Sea and the Indian Ocean (see Tillmann *et al.* 2014c). The most common situation reported so far in various regions was the detection of AZAs in shellfish before (if at all) the record of their causative organisms in the planktonic realm. In marine waters off Argentina the situation was different as the algae were known to occur a long time ago. A species of *Azadinium* caused at least three bloom episodes almost two decades ago (in 1990, 1991 and 1998), which were new events recorded on a global scale for these dinoflagellates (Akselman & Negri 2012; Akselman *et al.* 2014). Based on the presence of an antapical spine, the bloom species was designated as *Azadinium* cf. *spinosum*. However, for a final species designation, a few yet unresolved morphological details (e.g. presence of a ventral pore) of the Argentinean species need to be clarified. Generally, these reports of *Azadinium* from the South Atlantic showed a wide spatial distribution that encompassed northern Argentine and southern Uruguayan shelves including the mouth of Río de la Plata, and presented a marked seasonality in spring and autumn. Nevertheless, AZA toxins in shellfish were just recently reported but that could be because it had not been specifically looked for before. Anyhow, Turner and Goya (2015) for the first time reported low levels of AZA-2 in shellfish samples (*Brachidontes rodriguezii* and *Mesodesma mactroides*) from Argentina. This is in line with the first confirmation of the presence of AZA-2 producing *Azadinium* in the Argentinean coastal area by Tillmann *et al.* (2016), who isolated AZA-2 producing *Az. poporum* from coastal sediment samples. However, *Az. poporum* lacks an antapical spine and thus is clearly different from the species forming the dense 1990s blooms, so the question on the identity of the causative species of these blooms is still pending. In this paper we retrospectively focus on the 1991 episode with the conclusion that the causal organism – referred by Akselman and Negri (2012) as *Az.* cf. *spinosum* – in fact represents a new species. We also document the presence of other amphidomataceans during the bloom, a fact which supports the panorama of an ample geographical dispersion of this phylogenetic group also in the austral Southwest Atlantic region.

MATERIALS AND METHODS

Samples

Plankton samples were collected during an oceanographic cruise (R/V 'Cap. Oca Balda', OB-05/91, INIDEP) conducted along a transect of approximately 300 km from the coast to oceanic waters across the northern Argentine shelf in 12–13 September, 1991. Water samples were obtained by Niskin bottle casts and were fixed with Lugol's solution. Phytoplankton analysis here presented was performed on a surface sample from a station located in the core of the *Azadinium* bloom detected during the cruise, i.e. St 2 (38° 41′S, 56° 00′W) (see Akselman & Negri 2012; their fig. 1). After sedimentation in columns for quantitative studies, plankton material from a subsample was recovered and post-fixed with formalin (~2% final concentration) for storage until analysis.

Scanning electron microscopy

For Scanning electron microscopy (SEM), 0.5 mL of a dense concentrate of plankton material from a subsample of station two fixed in approximately 2% formalin was used. Cells were collected on polycarbonate filters (25 mm ∅, 3 μm pore-size, Merck Millipore, Billerica, USA) in a filter funnel where all subsequent washing and dehydration steps were carried out. Eight washings (2 mL deionized water each) were followed by a dehydration series in ethanol (30%, 50%, 70%, 80%, 95%, 100%; 10 min each). Filters were finally dehydrated with hexamethyldisilazane (HMDS), initially 1:1 HMDS:EtOH followed by 2 × 100% HMDS, and stored under gentle vacuum in a desiccator. Filters were mounted on stubs, sputtercoated (Emscope SC500, Ashford, UK) with gold-palladium and viewed under a scanning electron microscope (FEI Quanta FEG 200, Eindhoven, the Netherlands). SEM micrographs were presented on a black background using Adobe Photoshop 6.0 (Adobe Systems, San Jose, CA, USA).

RESULTS

Particulate matter size spectra and microscopic analysis of samples of the 1991 spring bloom here analyzed indicated that cells of an equivalent spherical diameter between 7.6 and 9.5 μm of a species provisionally considered as *Azadinium* cf. *spinosum*, was the dominant organism that caused high biomass values (Akselman & Negri 2012). Although the diatom *Thalassiosira anguste-lineata* (A. Schmidt) G. Fryxell & Hasle was a relevant species in the upper water

column along the area where the bloom of *Azadinium* occurred, it had a secondary importance in particulate matter concentration. In this study carried out with SEM on a representative sample of the bloom we focus on the nanoplankton size fraction to demonstrate the simultaneous presence of several species of the Amphidomataceae, which by their similar size and morphology in light microscopy (LM) had suggested to represent only one species. We also found that the most abundant species represents a new taxon which we describe below.

Taxonomic definition

Azadinium luciferelloides Tillmann et Akselman sp. nov.

Figs 1–5.

Description. Small thecate dinophyte, theca in SEM preparations 9.4–14.1 μm long and 7.6–11.6 μm wide. Epitheca conical, hypotheca flat and rounded, with a small antapical

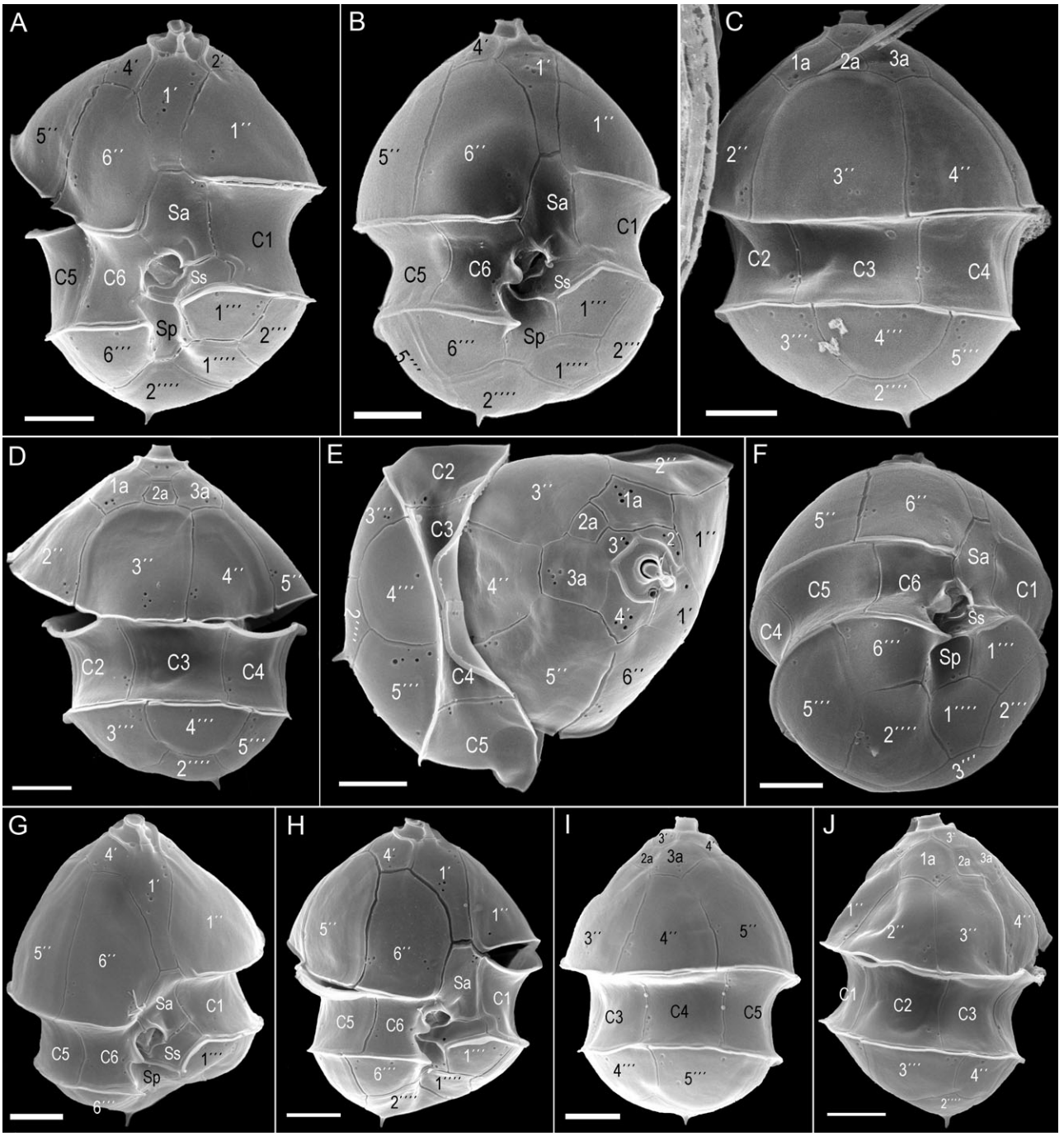

Fig. 1. Scanning electron micrographs (SEM) of *Azadinium luciferelloides* cells. (A, B) Ventral view, (C, D) dorsal view, (E) cell with epitheca in apical view, (F) ventral-antapical view, (G–I) right lateral view and (J) left lateral view. Scale bars = 2 μm.

spine. Plate tabulation: Po, cp, X, 4′, 3a, 6″, 6C, 5S, 6‴, 2⁗. A ventral pore located on the right ventral side in a notch of the pore plate.

Holotype. Cell shown in Fig. 1A, on SEM stub CEDiT2016H52 containing mixed plankton material (including also other amphidomatacean species reported below) from station 2 (38° 41′S, 56° 00′W). The stub is deposited at Senckenberg Research Institute and Natural History Museum, Centre of Excellence for Dinophyte Taxonomy, Germany.

Type locality. Argentinean middle shelf, approx. 150 km off the coast; coordinates: 38° 41′S, 56° 00′W.

Etymology. Luciferelloides: resembling a little Lucifer. The name here used as a specific epithet was originally chosen (as *Luciferella*) to designate what was considered to be a new genus after analysis of blooms from 1990 to 1991. Although initially communicated (Akselman 2001), the study was not published and the generic name was not mentioned to avoid incurring a 'nomen nudum' (Art. 38, McNeill et al. 2012, International Code of Nomenclature for algae, fungi, and plants 2012). *Luciferella*: from Lucifer (Latin), the Demon's name represented by value 666 in reference to the number of plates (6) in each of the contiguous series of precingular, cingular and postcingular plates.

Detailed description

Intact whole thecae of *Azadinium luciferelloides* observed with SEM were small, ovoid in shape, and slightly compressed dorso-ventrally (Fig. 1). The convex epitheca was higher than the hypotheca, and terminated in a conspicuous apical pore complex. The flat and generally rounded hypotheca bore a single small antapical spine which most commonly was slightly displaced and/or pointing to the cell's right side. The subequatorial cingulum was broad and conspicuous. Cell size as estimated from SEM pictures was 11.1 μm in length (±0.7 SD, range: 9.4–14.1 μm, $n = 182$). Cell width was slightly larger for the epitheca (9.1 ± 0.7 μm, range 7.6–11.6 μm, $n = 161$) than for the hypotheca (7.9 ± 0.6 μm, range 6.6–10.1 μm, $n = 164$) resulting in a mean length/width ratio of 1.4 or 1.2 when related to hypotheca or epitheca width, respectively.

The plate tabulation was determined as Po, cp, X, 4′, 3a, 6″, 6C, 5S, 6‴, 2⁗ and is schematized in Fig. 2. The epitheca consisted of six precingular plates, three anterior intercalary plates, four apical plates, and an apical pore complex. The first apical plate was rhomboid and only slightly asymmetric in its anterior part with contact with the 2′ plate smaller than the contact with the 4′ plate (Fig. 1A,B,G,H). The left-lateral apical plate 2′ was five sided and triangular in shape, whereas the right-lateral plate 4′ was six-sided and trapezoidal. The dorsal apical plate 3′ was hexagonal (Figs 1E, 3A,D). Of the three anterior intercalary plates, the left (1a) and right (3a) plates were relatively larger than the small and tetragonal mid intercalary plate 2a (Fig. 3A–D). The six precingular plates were roughly similar in size, with plate 1″ as the widest. Plate 1″ was in contact with an intercalary plate (1a) and thus in contact with four epithecal plates, whereas plate 6″ was separated from plate 3a by the apical plate 4′ (Fig. 3A).

The apical pore was ellipsoid (mean width: 0.81 ± 0.05 μm, mean length: 0.71 ± 0.05 μm, $n = 17$), located in the middle of the pore plate (Po), and covered by a cover plate (cp) (Fig. 3E–J). The pore plate was almost round with a mean diameter of 1.59 ± 0.08 μm ($n = 16$). A broad rim bordered the dorsal and lateral margins of the pore plate adjacent to apical plates 2′, 3′ and 4′, but was lacking ventrally, where the pore plate abutted the first apical plate and the X-plate. The cover plate was connected through a finger-like protrusion to the small X-plate, which slightly invaded the first apical plate (1′) with its posterior part. The X-plate, when seen from interior views of the cell (Fig. 3G), was small and round and slightly invaded the first apical plate. As a conspicuous part of the apical pore complex, a large (mean outer diameter: 0.33 ± 0.02 μm, $n = 19$) and distinct pore, designated as ventral pore (vp), was located at the right lateral side of the pore plate. This pore generally lay within a notch of the pore plate and contacted the first and the last apical plate (Fig. 3A,E–I). Rarely the vp was more shifted towards the first apical plate (Fig. 3J).

The hypotheca was composed by six postcingular and two antapical plates (Fig. 4A,B). From the postcingular plate series, plates 3‴ and 5‴ were the widest. Plates 1‴ and 6‴ were in ventral position. Postcingular plate 3‴ was in contact to both antapical plates. An oblique suture separated the two unequally sized antapical plates with the larger plate 2⁗ extending much more to the cells dorsal side and bearing the antapical spine.

The deeply concave sulcus (Fig. 4C–E) consisted of five plates. The large anterior sulcal plate (Sa) scarcely extended into the epitheca whereas the large posterior sulcal plate (Sp) extended about one-half of the line from the cingulum to the antapex. The left sulcal plate (Ss) was broad, located anterior to Sp and was running along the line from plate C1 to C6. Two smaller and centrally located sulcal plates (Sm and Sd) formed a concave central pocket. An additional structure was occasionally visible above Sm and Sd (Fig. 4D,E) but it could not be verified if this represented an additional sulcal platelet, or an internal outgrowth of plate C6 extending to both central sulcal plates. The deeply excavated and broad cingulum was composed of six plates of comparable size (Fig. 4B,F).

Thecal plates were smooth but most of them contained one or a few thecal pores (diameter: 0.11 ± 0.02 μm, range 0.07–0.16 μm, $n = 108$); the only plates always free of pores were the median intercalary plate 2a and the small central sulcal plates Sm and Sd. For the other plates both number and position of thecal pores was fairly conserved yielding a characteristic pattern as illustrated in Fig. 2. For example, on precingular plates pores were mainly found close to the cingulum and close to the sutures at underlapping margins. Exceptionally, on the keystone plate 3″, one or a cluster of a few pores were located in the middle of the plate, and both ventral precingular plates (1″ and 6″) had two groups of pores on the left and right side of the plate. The fairly high density of cells on the SEM stub allowed for a statistical analysis on the number of pores per plate (Fig. S3 in the Supporting Information).

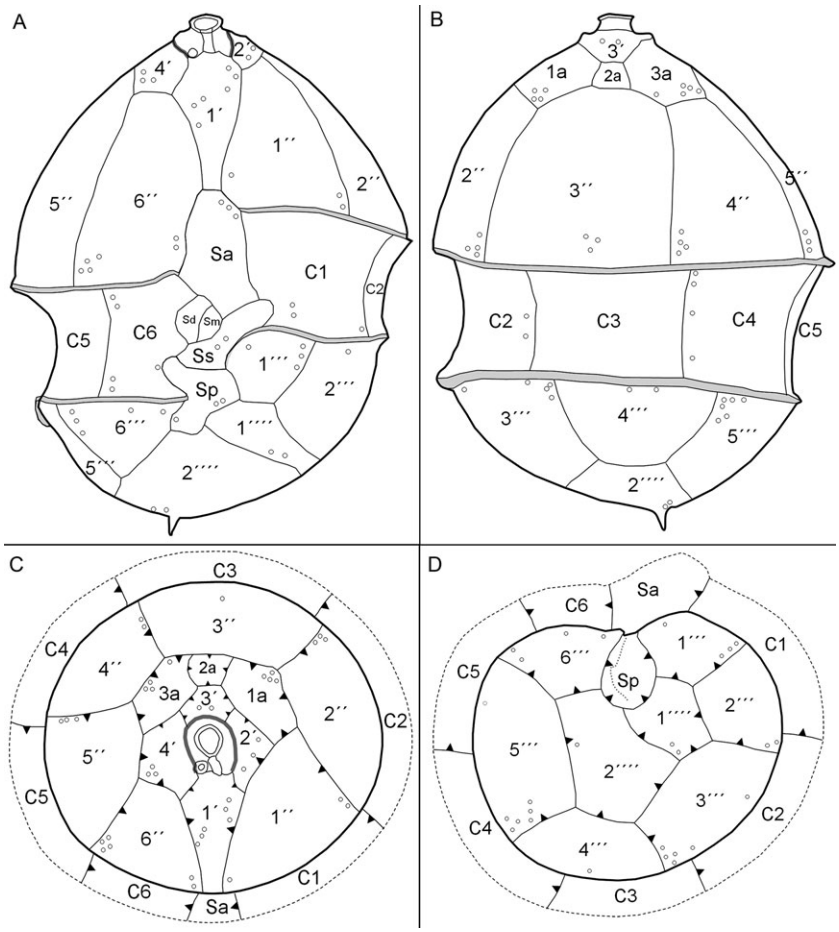

Fig. 2. Diagrammatic illustration of *Az. luciferelloides* thecal plates. (A) Ventral view, (B) dorsal view, (C) apical view and (D) antapical view. C, series of cingular plates; Sa, anterior sulcal plate; Sp, posterior sulcal plate; Ss, left sulcal plate; Sm, median sulcal plate; Sd, right sulcal plate. Grey circles: mean number and position of thecal pores. Arrowheads in (C) and (D) indicate plate overlap pattern.

Plate overlap pattern

Thecae with slightly disarranged plates, interior views, and the presence of growth bands (Fig. S1 in the Supporting Information) allowed an identification of the characteristic overlap patterns for thecal plate margins, which are schematized in Fig. 2C,D. Generally, overlap in epithecal, cingular and hypothecal plate series of *Azadinium luciferelloides* followed two general gradients: from dorsal to ventral and from cingulum to pole. As most notable features, plate 3′ was overlapped by its neighboring apical plates 2′ and 4′, plate 2a was overlapped by all adjacent plates, and plate C6 was overlapped by the anterior sulcal plate Sa. As keystone plates, i.e. plates that overlap all neighboring plates, we identified 3″, C3 and 4‴ for the precingular, the cingular, and the postcingular series, respectively.

Variability

The plate pattern and arrangement of *Azadinium luciferelloides* in the bloom field sample was rather stable; nevertheless, the shape of single plates was somewhat variable as exemplarily compiled in Fig. 5 (A–H, additional examples can be found in Fig. S2 in the Supporting Information) for the dorsal apical plates 3′ and 2a. Moreover, among the hundreds of cells inspected, a few aberrant plate patterns were observed (Fig. 5, see also Fig. S2 in the Supporting Information). The central small intercalary plate 2a, which normally was tetragonal and almost symmetrically located above plate 3″, was rarely observed to be in touch with the precingular plate 4″ (Fig. 5I,J) or even to be more diamond shaped and approaching a more symmetrical pentagonal shape and arrangement (Fig. 5K, Fig. S2 in the Supporting Information). Exceptionally, a 2a plate of this shape was displaced and not in touch to plate 3′ anymore (Fig. 5L). Other aberrant plate pattern included missing of a sulcal plate (Fig. 5O), or the presence of additional suture or aberrant arrangement within apical plates (Fig. 5M,N). Rarely cells with two small antapical spines were observed (Fig. 5P).

Other small Amphidomataceae

In addition to *Azadinium luciferelloides*, we identified a number of other Amphidomataceae in the sample (Figs 6–9). Specimens of *Az. spinosum* clearly could be identified by the characteristic position of the ventral pore, which was located in the middle of the first apical plate close to the suture of plate 1″ (Fig. 6). In addition, specimens identified as *Az. spinosum* based on the before mentioned character were slightly larger (theca in SEM preparation; length 13.4 ± 0.9 μm, hypotheca width 9.0 ± 0.7 μm; $n = 26$) than *Az. luciferelloides*, had a more slender shape, a longer hypotheca, larger intercalary plates, and had a significantly longer spine (0.84 ± 0.18, $n = 34$) when compared to the spine of *Az.*

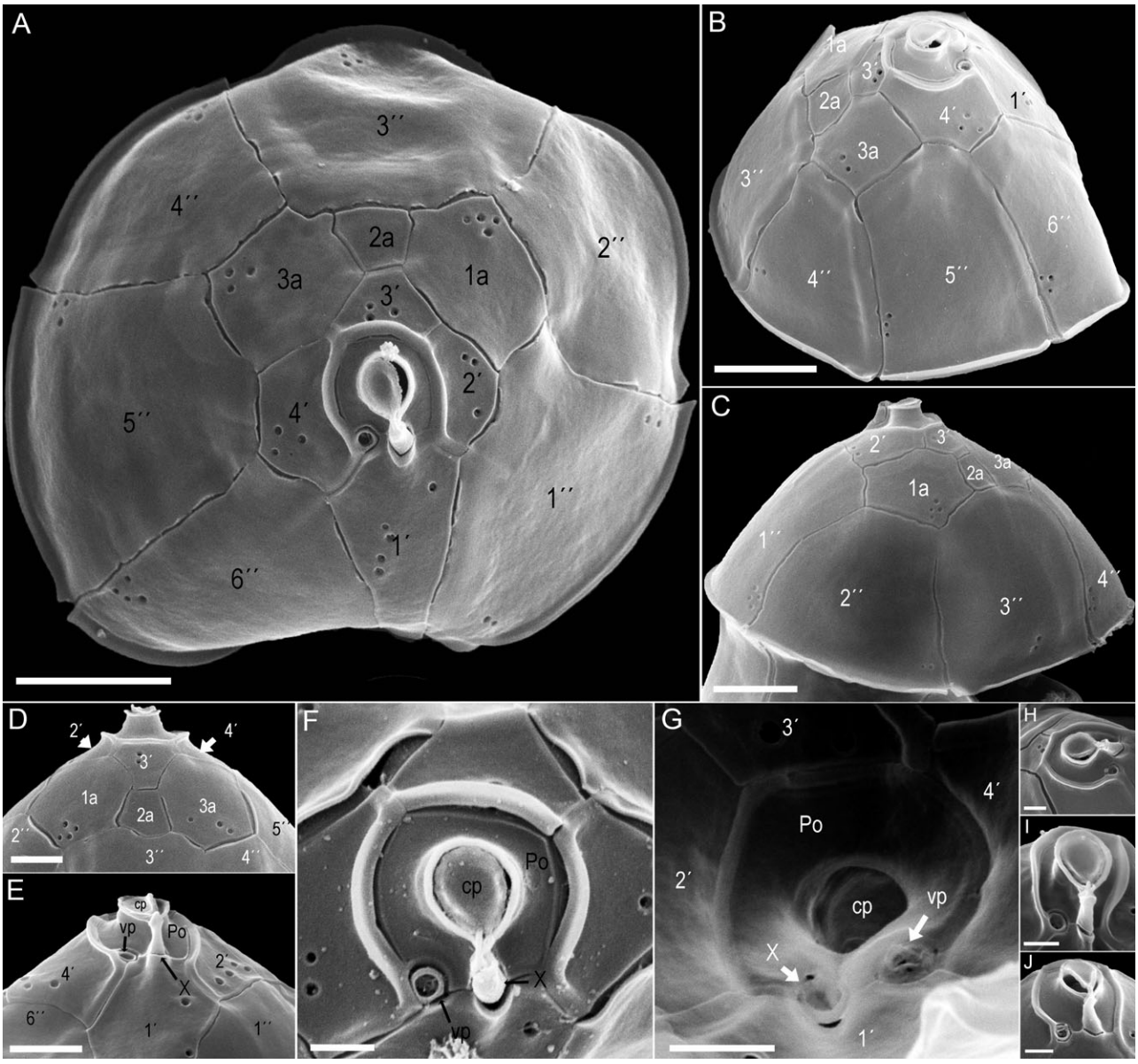

Fig. 3. SEM of *Az. luciferelloides* cells. (A) Apical view showing the complete series of epithecal plates. Epitheca in right lateral (B), left lateral (C), or dorsal (D) view. (E–J) Details of the apical pore complex (APC), (E) APC in ventral view, (F) APC in apical view, (G) APC viewed interiorly of the cell, (H) APC in right lateral view and (I, J) APC in ventral view. Po, pore plate; vp ventral pore; X, X-plate; cp, cover plate. Scale bars = 2 μm (A–C), 1 μm (D, E), or 0.5 μm (F–J).

luciferelloides (spine length 0.45 ± 0.07 μm, $n = 114$) (Student's t-test, $P < 0.005$).

The next species of small Amphidomataceae identified in the samples was *Az. dalianense* (Fig. 7). This identification was based on the combination of the following characters: presence of the ventral pore on the cells left side of the pore plate, presence of only three apical and only two anterior intercalary plates, and small size of the precingular plates 2″ and 4″. All cells identified as *Az. dalianense* had an antapical spine. Cell size, based on a few specimens only for which whole cell theca for size measurement was available, was 13.5 ± 0.6 μm in length and 9.2 ± 0.4 μm in width ($n = 6$).

Cells of *Az. dexteroporum* in the bloom sample (Fig. 8) were slightly smaller (theca in SEM preparation; length 8.6 ± 0.9 μm, hypotheca width 6.2 ± 0.5 μm; $n = 9$) compared to *Az. luciferelloides* and were mainly characterized by the ventral pore positioned at the cells right side of the pore plate at a slightly elongated tip of the pore plate, by small apical plates, and by a distinctly concave shape of the median intercalary plate 2a (Fig. 8B,D–F).

Amphidoma languida (theca in SEM preparation; length 10.6 ± 1.5 μm, hypotheca width 8.5 ± 0.9 μm; $n = 8$) was also present as identified by the characteristic row of six small apical plates, by the ventral pore on the apical right side of plate 1′, and by the large antapical pore on the second antapical plate (Fig. 9). One specimen with a reduction in apical plates (five instead of six, Fig. 9H) was observed.

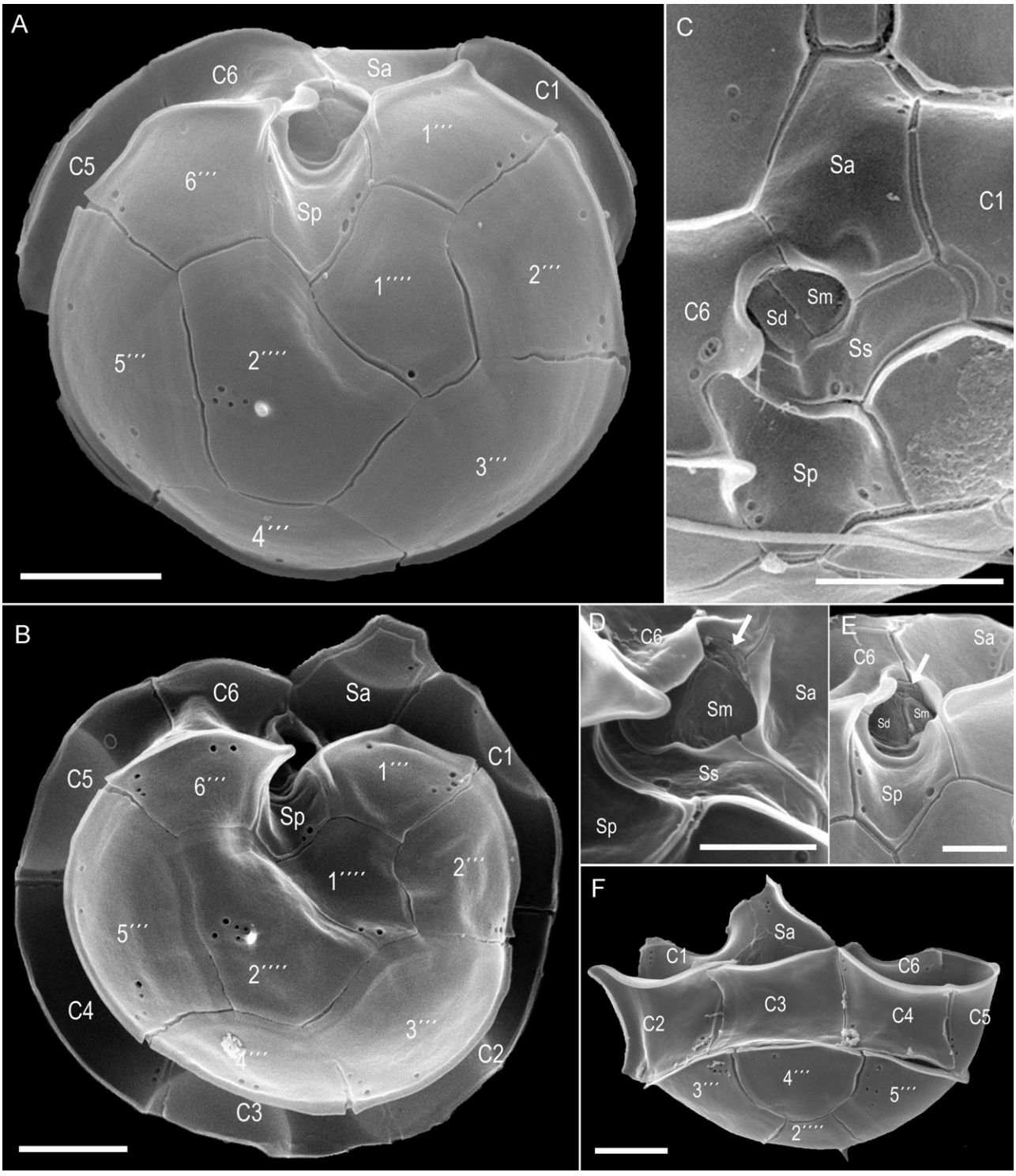

Fig. 4. SEM of *Az. luciferelloides* cells. (A, B) Antapical view of hypothecal plates, (C–E) details of the sulcal plate arrangement in ventral view. White arrow in (D, E) indicate an additional structure between plates Sm/Sd and C6. (F) Dorsal view of the hypotheca showing the series of cingular plates (C, series of cingular plates; Sa, anterior sulcal plate; Sp, posterior sulcal plate; Ss, left sulcal plate; Sm, median sulcal plate; Sd, right sulcal plate). Scale bars = 2 μm (A–C, F) or 1 μm (D, E).

Quantitative estimations

In total, the number of cells identified as *Azadinium spinosum*, *Az. dalianense*, *Az. dexteroporum*, and *Amphidoma languida* was 82, 23, 25 and 49, respectively. A few other yet undescribed species of both *Azadinium* and *Amphidoma* were identified in the sample in low numbers as well and will be described in more detail elsewhere. In order to

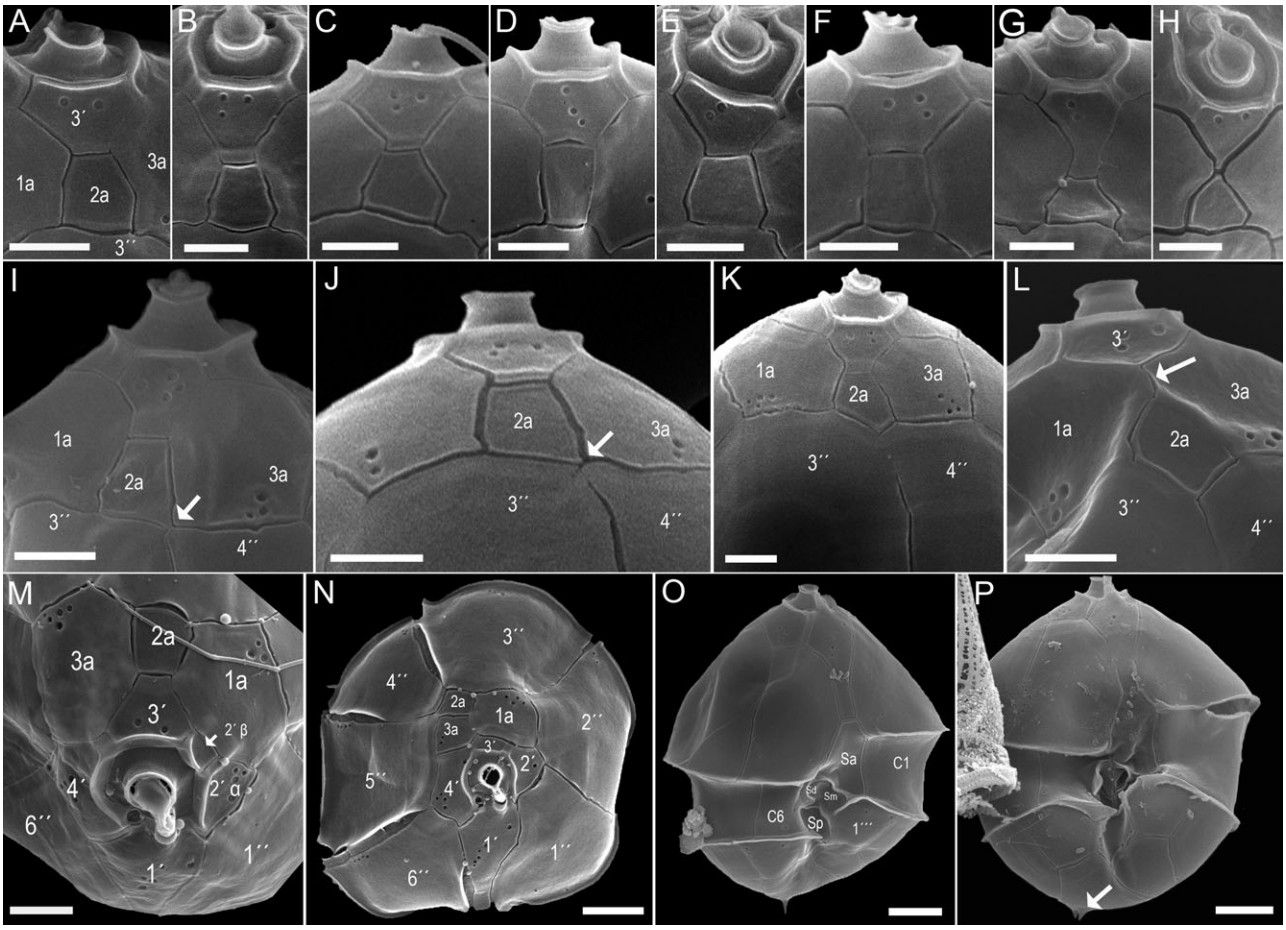

Fig. 5. SEM of *Az. luciferelloides* cells. (A–H) Variability in shape of the dorsal apical plates 3′ and 2a. (I–P) Variations in plate pattern. (I, J) Dorsal view of the epitheca showing plate 2a in minor contact with plate 4″ (white arrows). (K, L) Dorsal view of the epitheca with plate 2a in almost symmetric penta-configuration. Note that in (L) plate 2a is displaced and without contact to plate 3′(white arrow). (M, N) Apical view showing a subdivision of plate 2′ (M) or the anterior intercalary plates in an aberrant arrangement (N). (O) Whole cell in ventral view. Note that the sulcal plate Ss is missing (compare to Fig. 4C). (P) Ventral view of a cell with two small antapical spines (arrow). Scale bars = 1 μm (A–M) or 2 μm (N–P).

more quantitatively estimate the relative composition of the Amphidomataceae for the bloom sample, a part of the filter was systematically scanned and each cell was scored; among 970 cells of Amphidomataceae, 25% could not be assigned to a certain species (cells collapsed, wrinkled, *etc.*). From the others, 85.5% were identified as *Az. luciferelloides*, 6.5% as other small identified Amphidomataceae (*Az. spinosum*, *Am. languida*, *Az. dexteroporum*, *Az. dalianense*, the order reflects relative abundance), and 8.0% were assigned to other yet undescribed *Amphidoma*/*Azadinium* species. A previous estimation of the overall cell density in the surface sample of station two for cells of dimension and morphology which under LM resembled *Az.* cf. *spinosum* was 2.5×10^6 cells L^{-1}. Taking into account the percentages estimated by electron microscopy we calculated a cell density of approximately 2.14×10^6 cells L^{-1} for *Az. luciferelloides*, approximately 0.16×10^6 cells L^{-1} on the whole for *Az. spinosum*, *Am. languida*, *Az. dexteroporum* and *Az. dalianense*, and approximately 0.2×10^6 cells L^{-1} for the other *Amphidoma*/*Azadinium* species.

DISCUSSION

A 1991 spring bloom which caused high biomass values between 100 and 140 km offshore in middle shelf waters of northern Argentina was caused by a plankton population of a small species of *Azadinium* originally described as *Az.* cf. *spinosum* (Akselman & Negri 2012). The retrospective SEM analysis of archived bloom samples, however, now revealed the presence of several species of the Amphidomataceae and a clear dominance of a species of *Azadinium* described here as new.

There is no doubt that the new taxon belongs to the genus *Azadinium* as it conforms with all features described as characteristic for the genus, including the plate pattern with four apical and three epithecal intercalary plates, both six post- and precingular plates, and two antapical plates (Tillmann *et al.* 2009). Furthermore, the new taxon has the same arrangement of sulcal plates (with the plate Ss running across from the first to the last cingular plate) and of the apical pore complex (presence of an X-plate with a characteristic finger like

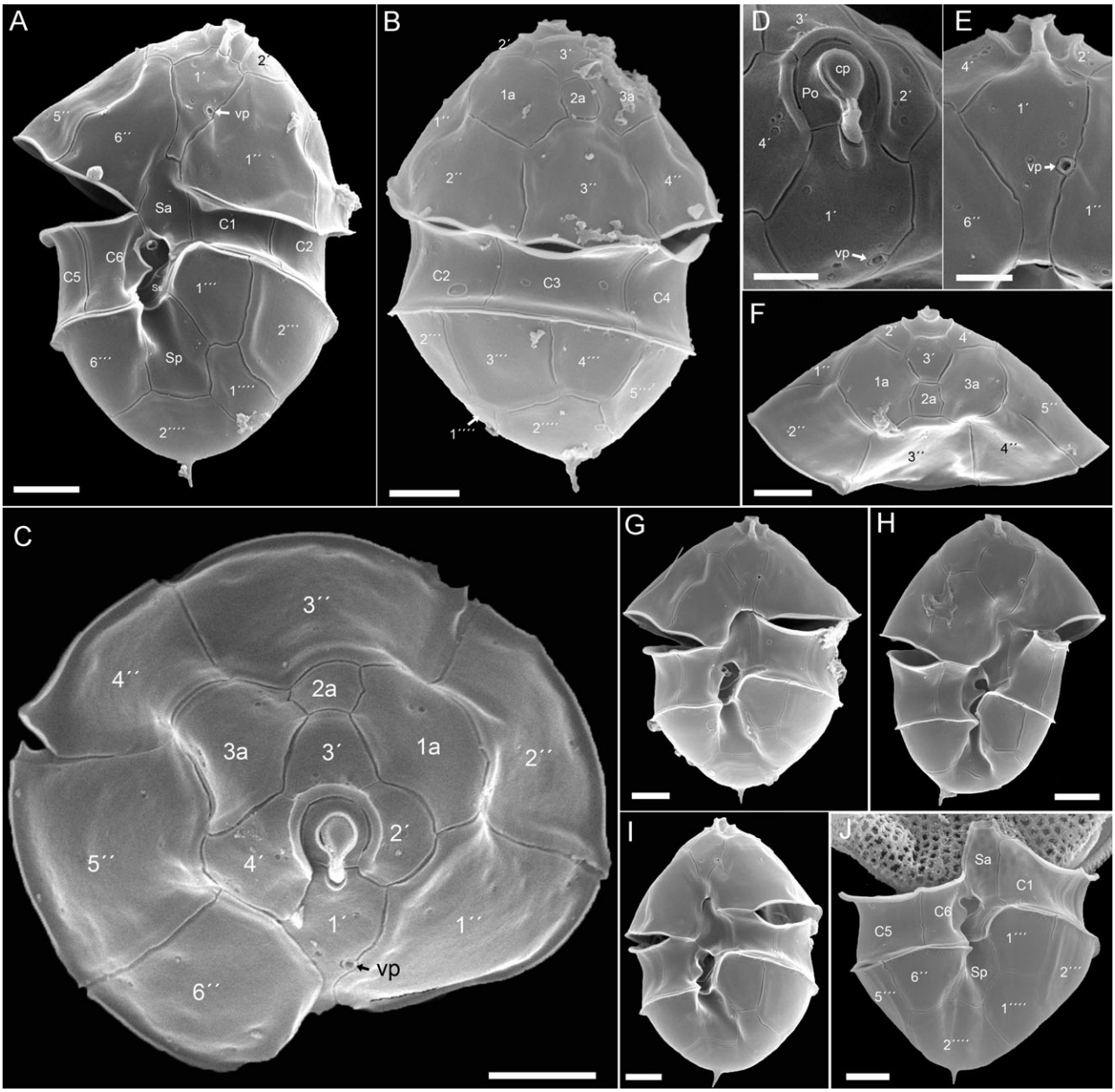

Fig. 6. SEM of *Az. spinosum* cells observed in the field sample. (A, B) Whole cells in ventral (A) and dorsal (B) view. (C) Apical view showing the complete series of epithecal plates. (D–F) Details of epithecal plates in apical/ventral (D), ventral (E), or dorsal (F) view. (G–I) Whole cells in ventral view and (J) hypotheca in ventral view. vp = ventral pore. Scale bars = 2 μm (A–C, F–J) or 1 μm (D, E).

extension connected to the cover plate), and the same plate overlap pattern characteristic for species of the Amphidomataceae (Tillmann *et al.* 2014a). Although *Az. luciferelloides* is similar to a number of other species of *Azadinium* in size and overall shape, it possesses distinctive and unique combination of features, which unambiguously differentiate this species from others. These mainly are the presence of an antapical spine, the size and shape of epithecal plates, the characteristic pattern in number and arrangement of thecal pores, and most distinctive, the location and arrangement of the ventral pore. Previous work on the 10 species of *Azadinium* described with both morphology and molecular data had shown that the phylogenetically well-separated species all differ in the position of the ventral pore. In all species the vp was always present and the position was stable, although in cultures very rarely (among hundreds of cells) a slightly deviating position of the ventral pore can be found (Potvin *et al.* 2012; Tillmann *et al.* 2014a). It is important to mention that two morphotypes of *Azadinium caudatum*, which have been differentiated at the variety level (Nézan *et al.* 2012), differed significantly in the vp position. At that time the position of the vp was considered not to be sufficient to separate the two morphotypes as two species. However, sequence data of both varieties differ significantly (Nézan *et al.* 2012) and ultimately breeding experiments are necessary to resolve the question if the two varieties in fact represent different species. In conclusion, we

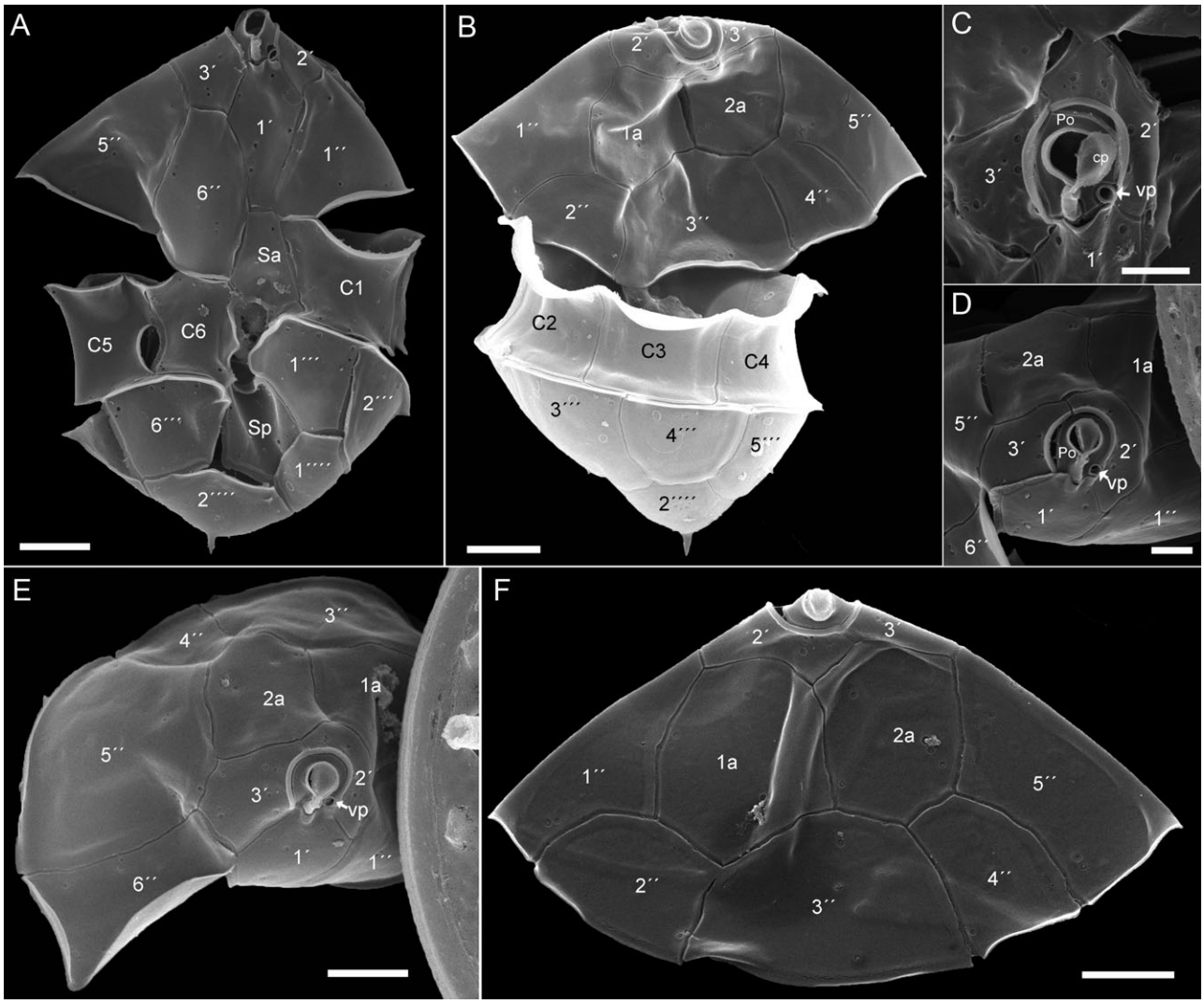

Fig. 7. SEM of *Az. dalianense* cells observed in the field sample. (A, B) Whole cell in ventral (A) or dorsal (B) view. (C–E) Apical view. Note the position of the ventral pore (vp) and the presence of three apical and two intercalary plates. (F) Epithecal plates in dorsal view. Note the presence of two intercalary plates and the small size of the precingular plates 2″ and 4″. Scale bars = 2 μm.

do consider the vp position as a significant morphological character for species separation of *Azadinium* and that the distinct vp position, together with a number of other characteristics, unambiguously differentiates *Az. luciferelloides* sp. nov. from other *Azadinium* as follows.

With the ventral pore on the cells right side of the pore plate, *Az. luciferelloides* is distinctly different from *Az. spinosum*, *Az. obesum* and *Az. polongum* (vp on the left side of plate 1′), from *Az. poporum*, *Az. dalianense*, *Az. trinitatum*, *Az. cuneatum* (vp on the left side of the pore plate), and *Az. caudatum* var. *caudatum* (vp on the right side of plate 1′) (see Table 3 in Tillmann *et al.* 2014a). Species that have a position of the vp cursory similar to *Az. luciferelloides* sp. nov. (on the cells right side of the pore plate) are *Az. caudatum* var. *margalefii*, *Az. concinnum*, and *Az. dexteroporum* (Tab. 1). *Azadinium caudatum* var. *margalefii* is different in size and shape, has a long spine sitting on a short horn (Table 1), and the vp is located inside of the pore plate without contact to the first apical plate (Fig. 10A). *Azadinium concinnum* is slightly smaller and more slender, and significantly differs from *Az. luciferelloides* by its large and symmetric precingular plates, by its very small epithecal intercalary plates, by its anterior elongated anterior sulcal plate, and by a different pattern of thecal pores (Tab. 1). Different to *Az. luciferelloides* (Fig. 10D), the location of the vp has a characteristic distortion of the suture Po/4′, the latter one characteristically accentuated by the recessed run of the rim (Fig. 10B). Like *Az. concinnum*, *Az. dexteroporum* is very small and has a pattern of thecal pores different to *Az. luciferelloides*. It clearly can be separated from *Az. luciferelloides* by its characteristic arrangement of the ventral pore, which is located at the right posterior end of the markedly asymmetric pore plate (Table 1, Fig. 10C). In terms of cell size it has to be kept in mind that size of *Az. luciferelloides* has been estimated from SEM images only. Cells dehydrated during SEM preparation can significantly shrink causing a significant difference in mean size measurements using LM and SEM (Salas *et al.* 2014) and thus size of live *Az. luciferelloides* probably is larger than listed in Table 1.

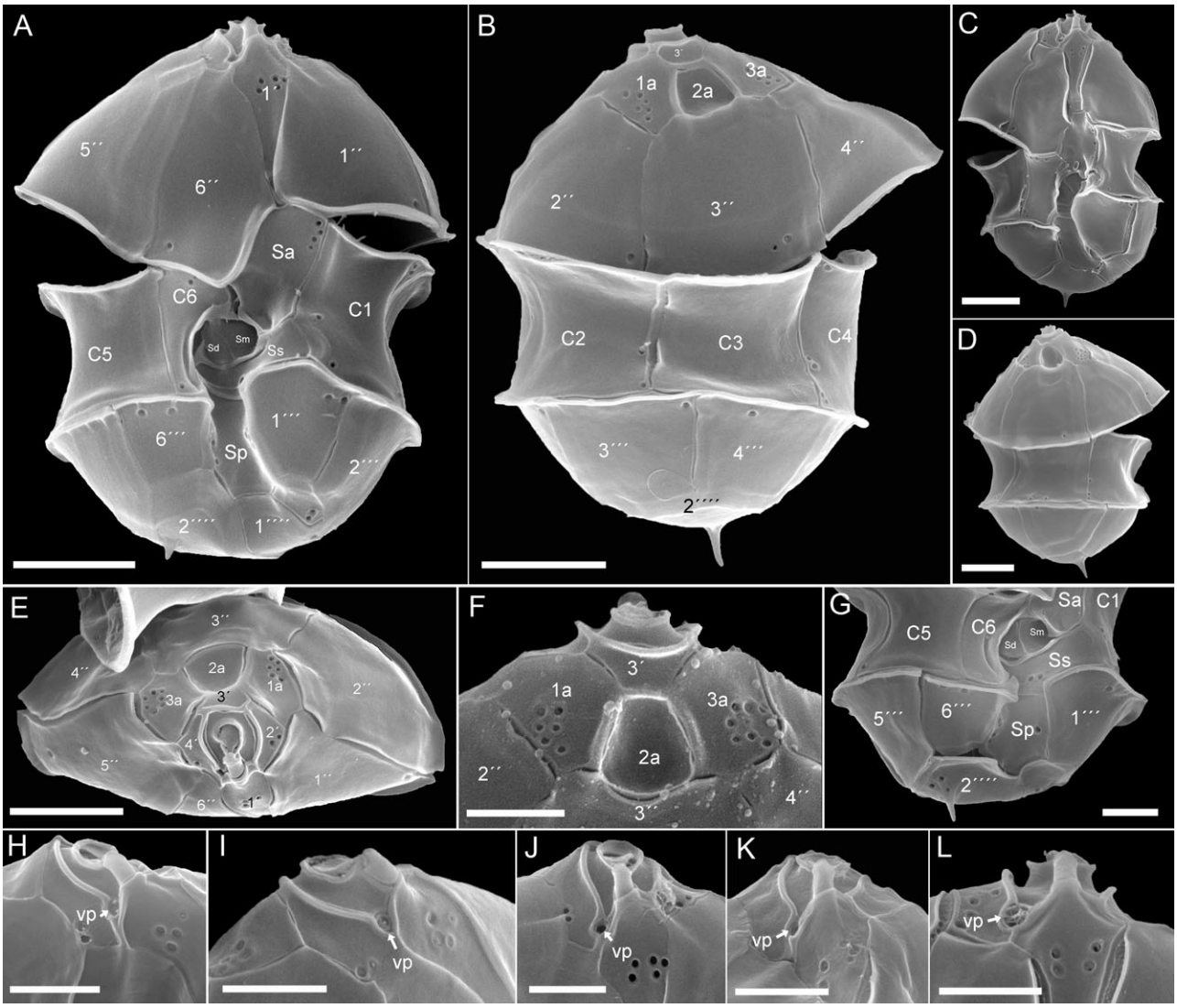

Fig. 8. SEM of *Az. dexteroporum* cells observed in the field sample. (A–D) Whole cells in ventral (A, C) or dorsal (B, D) view. (E) Epitheca in apical view, (F) epitheca in dorsal view. Note the concave shape of plate 2a. (G) Hypotheca in ventral view. (H–L) Apical pore complex in right lateral (H, I) or ventral (J–L) view to illustrate the position of the ventral pore (vp). Scale bars = 2 μm (A–E) or 1 μm (F–L).

The awareness that several similar species of *Azadinium* and *Amphidoma* were present in the sample has some implications. All the amphidomatacean species, which we here identified in the sample are too similar in general size and shape to be reliably identified in the light microscope. We thus, at the moment, are not able to provide LM pictures/description of the species *Az. luciferelloides* highlighting basic cellular features like type, number and position of chloroplast, or shape and position of nucleus and/or the presence and location of pyrenoid(s). There are published LM micrographs from cells of the 1990 bloom (which might be assumed to be dominated by *Az. luciferelloides* as well) designated as *Az.* cf. *spinosum* (Akselman & Negri 2012), but there are no archived samples of this bloom available that might allow a SEM determination of the 1990 species. We also do not know if the 1998 bloom was multispecific as the 1991 was, but the dominant phenotype at the LM was as well that of *Az.* cf. *spinosum* (Akselman *et al.* 2014). There are some unpublished LM micrographs of 1991 bloom samples, but here we cannot with certainty link a LM micrograph to a certain species. Nevertheless, all old LM observations had shown that all cells of *Azadinium* of Argentinean bloom samples had chloroplast making it highly likely that the dominant *Azadinium* species, *Az. luciferelloides*, is – like all other species of *Azadinium* – photosynthetic. However, cultures of *Az. luciferelloides* are needed to determine these basic cellular features.

Azadinium is a relatively young genus and all species descriptions up to now have been based on both morphology and molecular sequence information. This was possible because for almost all taxa (*Az. caudatum* var. *caudatum* as the exception), cultures were available. *Azadinium luciferelloides* now is the first species of *Azadinium* for which no molecular sequence data could be provided. Phytoplankton species are traditionally defined according to morphological features, but molecular data are becoming more and more a standard complementing algal species delimitation and for

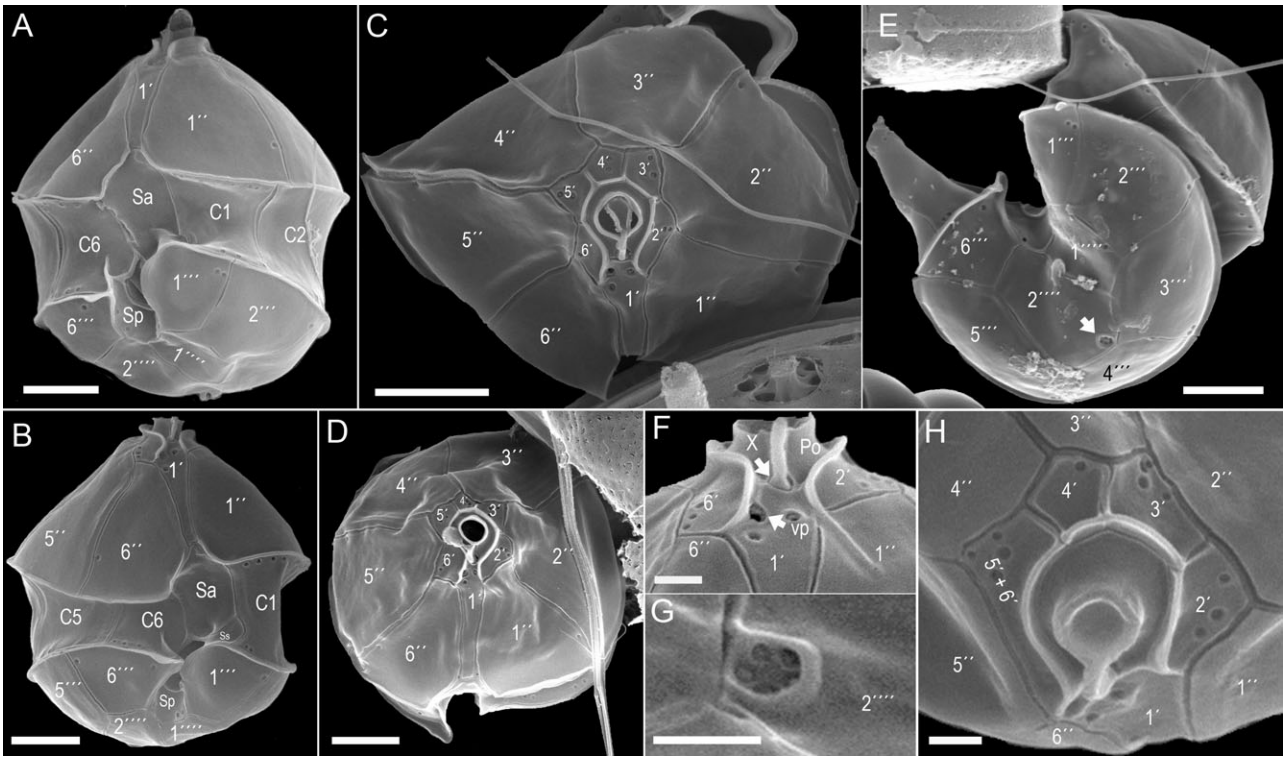

Fig. 9. SEM of *Amphidoma languida* cells observed in the field sample. (A, B) Whole cells in ventral view, (C, D) epitheca in apical view, (E) hypotheca in antapical view. Note the large antapical pore (arrow). (F) Detailed view of the apical pore complex showing the position of the ventral pore (vp) and the X-plate (X), (G) detailed view of the large antapical pore located on the second antapical plate and (H) apical view showing the presence of five apical plates (fusion of plate 5′ and 6′). Scale bars = 2 μm (A–E) or 0.5 μm (F–H).

testing traditional species boundaries (Leliaert *et al.* 2014). It thus has become rare for extant species to be defined solely by morphology. Nevertheless, in the Dinophyceae, at least six of the 76 new species descriptions since 2010 (number of new species according to www.dinophyta.org accessed October 2015) have solely been based on morphology. The majority of these last 5 years dinophycean species descriptions are based on cultures (46 of 76), and for others (mainly larger unculturable species) sequence information is usually retrieved from single cell qPCR. In case of our available material of *Az. luciferelloides*, this approach has been unfeasible because of the long-term sample storage in formalin. Moreover, and more importantly, in case of small and inconspicuous species such as those of *Azadinium* it is virtually impossible to first unambiguously determine the identity of specimens subsequently used for single cell qPCR. Though a method has been described where DNA was extracted from single cells whose morphology had previously been fully characterized by electron microscopy (Takano & Horiguchi 2005). However, this method obviously is limited to larger cells, and since its description using two large dinophycean species, has never been successfully applied. For small species of the Amphidomataceae, establishing unialgal cultures is thus the only mean to unequivocally link morphology and sequence information and/or other important phenotypic characteristics like AZA production. However, isolation and growth of small and inconspicuous algal species is a difficult task and up to now no cultures of *Az. luciferelloides* could be established. Cyst hatching experiments with sediment from the coastal El Rincón area (Buenos Aires Province) successfully yielded cultures of *Azadinium*, but without exception these were *Az. poporum* (Tillmann *et al.* 2016). Accessing the more offshore 1991 bloom area of the Argentinean shelf break for live plankton sampling and culture establishment is logistically even more difficult, but nevertheless we will continue to attempt to get hands on cultures of *Az. luciferelloides* in the future.

Species descriptions based solely on morphology may be problematic for two reasons: (i) Morphologically different cells might represent different stages of a common life cycle. (ii) Species descriptions based on just one or very few specimens fail to evaluate the natural variability of the morphological character(s) used to separate a new taxon from others. In case (i) it is quite unlikely that *Az. luciferelloides* is a live cycle stage of one of the described *Azadinium* species as this taxon was dominant in abundance, whereas gametes or zygotes of the Dinophyceae normally are rare. With respect to natural variability (ii), our conclusion is based on the observation of a large number (>500) of cells, which allowed us to catch the range of variability, e.g. in the shape of certain plates (Fig. 5A–H, Fig. S2 in the Supporting Information) and/or the number and position of small pores on each of the thecal plates (Fig. S3 in the Supporting Information). The latter was found to vary in a relatively narrow range, but more data for other species are needed before the pattern of thecal pores might be more widely used as a supplementary species-specific morphological descriptor.

Table 1. Compilation of morphological features of species of *Azadinium* (including *Az. luciferelloides*) with a ventral pore located on the cells right side of the pore plate. For morphological features of other amphidomatacean species see Table 2 in Tillmann *et al.* (2014a).

	Az. caudatum var. *margalefii*	*Az. dexteroporum*	*Az. concinnum*	*Az. luciferelloides*
Length range (mean)	25.0–42.1 μm	7.0–10.0 (8.5) μm	8.0–11.5 (9.5) μm	9.4–14.1† (11.1) μm
Width range (mean)	18.4–30.0 μm	5.0–8.0 (6.2) μm	5.6–8.3 (6.6) μm	6.6–10.1† (7.9) μm
Length/Width ratio	1.2	1.4	1.4	1.4
Antapical projection	Short horn, long spine	Spine	Spine	Spine
Stalked pyrenoid	None	1	None	Unknown
1″ adjacent to 1a	Yes	Yes	No	Yes
Ventral pore position	Pore plate, right side, inside Po	End of pore plate, right side	Pore plate, right side	Pore plate, right side
Pore plate symmetry	Suture to 1′ almost symmetric	Suture to 1′ strongly asymmetric, left side more apical	Suture to 1′ almost symmetric	Suture to 1′ almost symmetric
Relative size first and last intercalary	Small	Small	Very small	Small
Relative size apical plates	Medium	Small	Small	Small
Pattern of thecal pores	Many scattered pores	Pores in quite fixed positions. E.g. postcingular plates with one (or very few) pores close to the underlapping margins; keystone plate 4‴ without pores	Very few pores in quite fixed positions. No pores on precingular plates, postcingular plates with one (or very few) pores close to the underlapping margins, keystone plate 4‴ without pores	Few and well defined number of pores on each plate (see Fig. S1 in the Supporting Information) different to the other species, e.g. 4–7 pores on plate 5‴, keystone plate 4‴ with 1 to 2 pores
Records	Mediterranean, North Sea, Atlantic	Mediterranean, North Atlantic, South Atlantic	North Atlantic	South Atlantic
References‡	a, b	c, d	e	This study

†Based on SEM only.
‡a, Nézan *et al.* (2012); b, Tillmann *et al.* (2014b); c, Percopo *et al.* (2013); d, Tillmann *et al.* (2015); e, Tillmann *et al.* (2014a).

Generally, evaluation of morphological variability is always difficult with field samples when several different but similar species are present. The morphological species concept uses discontinuities in morphological variation to distinguish species (Leliaert *et al.* 2014). The position of the ventral pore for *Azadinium* very clearly satisfies this criterion. Among all the cells of small Amphidomataceae in the sample, there were differences in vp position, but these were discrete, without any intermediate stages, and conformed with other morphological details showing the presence of several *Azadinium* species. For a few specimens of *Az. luciferelloides* in the field sample there was a deviant or aberrant pattern of plates, as has been described for cultured cells of many other *Azadinium* species (e.g. Tillmann *et al.* 2010). For a clonal culture of *Az. cuneatum*, the presence of both quadra- and penta-configuration of plate 2a has been described (Tillmann *et al.* 2014a). Based on this knowledge on the intraspecific variability of a closely related well-described species, the *Az. luciferelloides* cells, e.g. depicted in Fig. 5K,L, albeit their distinctly different arrangement of plate 2a, were of course not regarded as 'new' species.

A main finding of this study is that, in addition to the abundant and dominant *Az. luciferelloides*, a number of other small species of the Amphidomataceae were present. For each of the species the conclusion was based on the identification of a large number of specimens by the specific combination of features characteristic for the respective species.

With the position of the vp, with a slender cell shape and with a well-developed spine, cells identified as *Az. spinosum* were concordant with the original description (Tillmann *et al.* 2009). *Az. dalianense*, with only three apical plates and two intercalary plates (Luo *et al.* 2013), cannot be misidentified when epithecal plates are visible. It should be noted that all cells identified here as *Az. dalianense* had a short antapical spine. For a cultured Chinese strain of *Az. dalianense* in the original species description this trait was found to be unstable, with only 18% of cells having a spine (Luo *et al.* 2013). Thus, targeted studies are needed to evaluate potential effects of environmental and culture conditions on spine formation and other morphological features of *Azadinium*. All cells with a left sided vp, for which epithecal plates and/or the hypotheca were simultaneously visible, had '*dalianense*' characteristics. Nevertheless, for a few cells the vp but not the epithecal plates and/or the hypotheca was visible. We thus cannot exclude the presence of *Az. poporum*, which has an arrangement of the vp only slightly different from *Az. dalianense* (Tillmann *et al.* 2011). In fact, *Az. poporum* has recently been raised from sediment samples collected from the Argentinean coastal area (Tillmann *et al.* 2016). Cells identified as *Az. dexteroporum* conform to the original species description based on a Mediterranean strain (Percopo *et al.* 2013). As has been emphasized for the type material, the central intercalary plate 2a of *Az. dexteroporum* in the Argentinean sample was concave. This is interesting to note as this

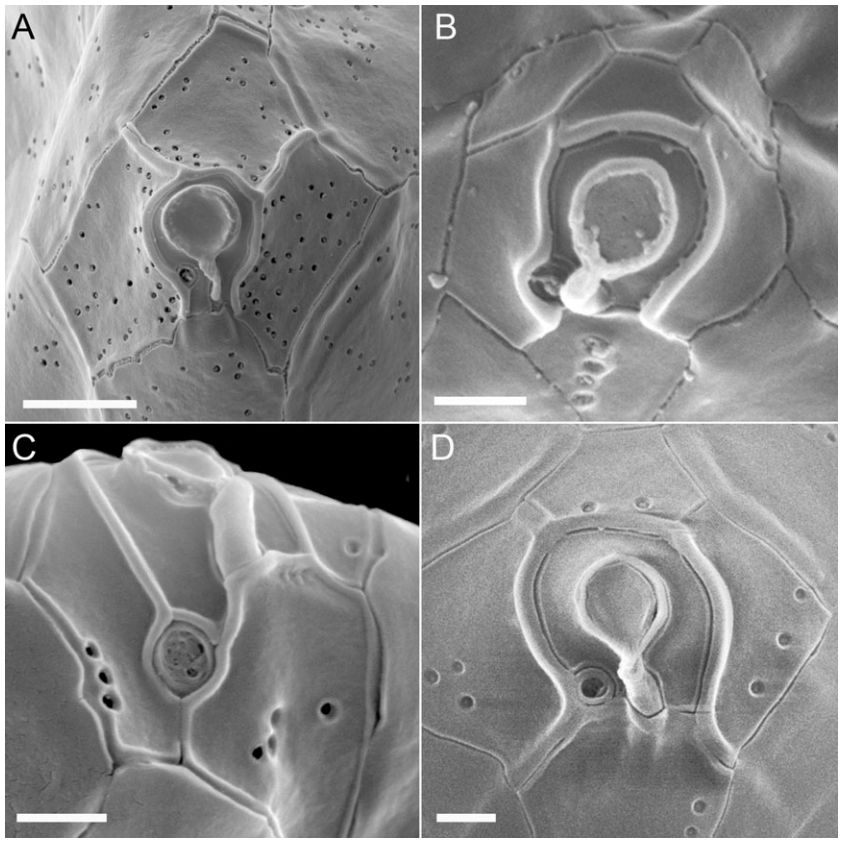

Fig. 10. Comparative view of the apical pore complex and the position of the ventral pore (vp) of four species of *Azadinium* which have the vp located on the cells right side of the pore plate. (A) *Az. caudatum* var. *margalefii*, (B) *Az. concinnum*, (C) *Az. dexteroporum* and (D) *Az. luciferelloides*. Scale bar = 2 μm (A) or 0.5 μm (B–D).

plate was plain for a recently described subarctic strain of *Az. dexteroporum* from the Irminger Sea (Tillmann *et al.* 2015). This subarctic isolate differed significantly in terms of ITS genetic distance ($p = 0.04$) from the Mediterranean *Az. dexteroporum* strain indicating some cryptic diversity for this species, and it thus would be desirable to have molecular information of the Argentinean *Az. dexteroporum*. *Amphidoma languida* was common in the samples as well. Forty-nine cells could be unambiguously identified by the presence of six small apical plates, a vp on the anterior right side of 1′, and a large antapical pore on the larger antapical plate 2′′′′. All cells identified as *Am. languida* had the typical pattern of thecal pores with one (very rarely up to three) pore consistently located at the underlapping sutures of pre- and postcingular plates and with the keystone plates (i.e. plates that overlap all adjacent plates) free of pores (Tillmann *et al.* 2012a).

The identification of *Az. spinosum*, *Az. dalianense*, *Az. dexteroporum* and *Am. languida* are the first record of these species for the South Atlantic and thus describe an important range extension of the species. Furthermore it strongly supports the previous notion that several species of *Azadinium* do co-occur (Tillmann *et al.* 2010, 2011, 2014a; Nézan *et al.* 2012). Such a co-existence of potentially toxigenic (e.g., *Az. spinosum*, *Az. dexteroporum*) and non-toxigenic species (e.g., *Az. dalianense*) in the same water mass complicate all attempts to identify/quantify the source organism of AZAs by routine monitoring programs using LM. Thus, there is an urgent need for molecular tools to routinely detect and discriminate species of *Azadinium*/*Amphidoma*, some of which have successfully been developed in the past (Toebe *et al.* 2013; Smith *et al.* 2016).

With the identification and clarification of the dominant bloom forming species of the 1991 episode and with a first record of four other species of the Amphidomataceae for Argentinean shelf blooms, our study provides a significant taxonomic advancement. However, the AZA toxin production potential of the local species/populations still needs to be clarified. The species *Az. spinosum*, *Az. dexteroporum* and *Am. languida* are known as AZA producers (Tillmann *et al.* 2009; Krock *et al.* 2012; Percopo *et al.* 2013), but with a limited number of available cultured strains it is still not entirely clear if and to what extent AZA production is a species-specific stable phenotypic trait. For *Az. spinosum*, there is evidence that this might be the case; all four available isolates have the same AZA profile consisting of AZA-1, -2, and -33 (Salas *et al.* 2011; Tillmann *et al.* 2012b). In contrast, *Az. poporum* has been shown to be more variable: whereas all three available North Sea isolates produce AZA-37 (Krock *et al.* 2012), *Az. poporum* from the Asiatic Pacific region produces more complex AZA profiles including AZA-2, -11, -36, -40, -41 in different combinations, and also strains without any known AZAs have been described (Gu *et al.* 2013; Krock *et al.* 2014). For *Az. dexteroporum*, the presence of AZAs has been unambiguously described for the Mediterranean isolate (Percopo *et al.* 2013). However, a new strain of *Az. dexteroporum*, isolated from the subarctic Irminger Sea clearly lacked any of these or other known AZAs (Tillmann *et al.* 2015). These examples clearly show that in Argentina there is an urgent need to obtain local strain cultures of the Amphidomataceae to clarify their AZA production potential.

The 1991 bloom, like other blooms of *Azadinium* described for 1990 and 1998 (Akselman & Negri 2012;

Akselman *et al.* 2014), developed in the middle shelf and the shelf-break areas during the spring phytoplanktonic productive period. In 1990 there were also records of its blooms at the coastal front of El Rincón (Akselman & Negri 2012). The extended shelf break front of the Argentine Sea during spring and summer is a highly productive area rich in exploited marine resources. Blooms of *Azadinium* therefore represent an important input to both the planktonic and benthic food web (Akselman & Negri 2012). Natural beds of *Zygochlamys patagonica* (Patagonian scallop) spreading along the Argentinean continental shelf (Bogazzi *et al.* 2005) are commercially exploited. In addition, wild beds of mollusks from intertidal and subtidal zones have been traditionally harvested by fishermen and some companies have begun to improve the culture of oysters and mussels along the coast from the South of Buenos Aires, North Patagonian Gulfs and Tierra del Fuego (Pascual & Zampatti 1999; Medina *et al.* 2011). Together with the first records of AZAs in Argentinean shellfish (Turner & Goya 2015) this underlines the need for more data on the AZA production potential of Amphidomataceae species locally present in order to fully evaluate the risk potential of AZA shellfish contamination episodes in the Southwestern Atlantic region.

ACKNOWLEDGEMENT

We thank Professor Santiago Bassano (Mar del Plata, Argentina) for help with Latin in an early stage of this study. This is Contribution No. 1973 of the Instituto Nacional de Investigación y Desarrollo Pesquero (INIDEP), Mar. del Plata, Argentina.

REFERENCES

Akselman, R. 2001. Un nuevo dinoflagelado (Peridiniales, Dinophyceae) causante de discoloraciones en el Atlántico Sudoccidental. *Bol. Soc. Argent. Bot.* **36**: 55.

Akselman, R. and Negri, R. M. 2012. Blooms of *Azadinium* cf. *spinosum* Elbrächter et Tillmann (Dinophyceae) in northern shelf waters of Argentina, Southwestern Atlantic. *Harmful Algae* **19**: 30–8.

Akselman, R., Negri, R. M. and Cozzolino, E. 2014. *Azadinium* (Amphidomataceae, Dinophyceae) in the Southwest Atlantic: *in situ* and satellite observations. *Rev. Biol. Mar. Oceanogr.* **49**: 511–26.

Álvarez, G., Uribe, E., Avalos, P., Marino, C. and Blanco, J. 2010. First identification of azaspiracid and spirolides in *Mesodesma donacium* and *Mulinia edulis* from Northern Chile. *Toxicon* **55**: 638–41.

Amzil, Z., Sibat, M., Royer, F. and Savar, V. 2008. First report on azaspiracid and yessotoxin groups detection in French shellfish. *Toxicon* **52**: 39–48.

Bogazzi, E., Baldoni, A., Rivas, A. *et al.* 2005. Spatial correspondence between areas of concentration of Patagonian scallop (*Zygochlamys patagonica*) and frontal systems in the southwestern Atlantic. *Fish. Oceanogr.* **14**: 359–76.

Braña Magdalena, A., Lehane, M., Krys, S., Fernández, M. L., Furey, A. and James, K. J. 2003. The first identification of azaspiracids in shellfish from France and Spain. *Toxicon* **42**: 105–8.

Colman, J. R., Twiner, M. J., Hess, P. *et al.* 2005. Teratogenic effects of azaspiracid-1 identified by microinjection of Japanese medaka (*Oryzias latipes*) embryos. *Toxicon* **45**: 881–90.

Furey, A., O'Doherty, S., O'Callaghan, K., Lehane, M. and James, K. J. 2010. Azaspiracid poisoning (AZP) toxins in shellfish: toxicological and health considerations. *Toxicon* **56**: 173–90.

Gu, H., Luo, Z., Krock, B., Witt, M. and Tillmann, U. 2013. Morphology, phylogeny and azaspiracid profile of *Azadinium poporum* (Dinophyceae) from the China Sea. *Harmful Algae* **21–22**: 64–75.

Guiry, M. D. 2015. Amphidoma. *In* Guiry, M. D. G. and M., Guiry G. (Eds.) *AlgaeBase*. National University of Ireland, Galway. Worldwide electronic publication. (taxonomic information republished from AlgaeBase with permission of M. D. Guiry). Accessed through: World Register of Marine Species. [Cited on 15 October 2015]. Available from: http://www.marinespecies.org/aphia.php?p=taxdetails&id=109517.

Hernández-Becerril, D. U., Barón-Campis, S. A. and Escobar-Morales, S. 2012. A new record of *Azadinium spinosum* (Dinoflagellata) from the tropical Mexican Pacific. *Rev. Biol. Mar. Oceanogr.* **47**: 553–7.

Hess, P., McCarron, P., Krock, B., Kilkoyne, J. and Miles, C. O. 2014. Azaspiracids: chemistry, biosynthesis, metabolism, and detection. *In* Botana, L. M. (Ed.) *Seafood and Freshwater Toxins*. CRC Press, Boca Raton, FL, pp. 799–821.

James, K. J., Furey, A., Lehane, M. *et al.* 2002. First evidence of an extensive northern European distribution of azaspiracid poisoning (AZP) toxins in shellfish. *Toxicon* **40**: 909–15.

James, K. J., Moroney, C., Roden, C. *et al.* 2003. Ubiquitous "benign" alga emerges as the cause of shellfish contamination responsible for the human toxic syndrome, azaspiracid poisoning. *Toxicon* **41**: 145–54.

Kaufmann, M. J., Santos, F. and Maranhao, M. 2015. Checklist of nanno- and microplankton off Madeira Island (Northeast Atlantic) with some historical notes. *Nova Hedwigia*. doi: 10.1127/nova_-hedwigia/2015/0265.

Krock, B., Tillmann, U., John, U. and Cembella, A. D. 2009. Characterization of azaspiracids in plankton size-fractions and isolation of an azaspiracid-producing dinoflagellate from the North Sea. *Harmful Algae* **8**: 254–63.

Krock, B., Tillmann, U., Voß, D. *et al.* 2012. New azaspiracids in Amphidomataceae (Dinophyceae): proposed structures. *Toxicon* **60**: 830–9.

Krock, B., Tillmann, U., Witt, M. and Gu, H. 2014. Azaspiracid variability of *Azadinium poporum* (Dinophyceae) from the China Sea. *Harmful Algae* **36**: 22–8.

Leliaert, F., Verbruggen, H., Vanormelingen, P. *et al.* 2014. DNA-based species delimitation in algae. *Eur. J. Phycol.* **49**: 179–96.

López-Rivera, A., O'Callaghan, K., Moriarty, M. *et al.* 2010. First evidence of azaspiracids (AZAs): a family of lipophilic polyether marine toxins in scallops (*Argopecten purpuratus*) and mussels (*Mytilus chilensis*) collected in two regions of Chile. *Toxicon* **55**: 692–701.

Luo, Z., Gu, H., Krock, B. and Tillmann, U. 2013. *Azadinium dalianense*, a new dinoflagellate from the Yellow Sea, China. *Phycologia* **52**: 625–36.

Massucatto, A., Siqueira Pilotto, A. L. and Schramm, M. A. 2014. *Investigação da presença de Azaspirácidos em recursos pesqueiros do Canal do Linguado*. SEPEI, Instituto Federal, Santa Catarina, ISSN 2357-836X.

McMahon, T. and Silke, J. 1996. West coast of Ireland; winter toxicity of unknown aetiology in mussels. *Harmful Algae News* **14**: 2.

McNeill, J., Barrie, F. R. and Buck, W. R. *et al.* (Eds). 2012. International Code of Nomenclature for algae, fungi, and plants (Melbourne Code). [Cited on 15 November 2015]. Available from: http://www.iapt-taxon.org

Medina, D., Goya, A. B. and Rozas, C. 2011. Molluscan shellfish safety in South America. *In* Sauvé, G. (Ed.) *Molluscan Shellfish Safety*. Springer, Dordrecht, Heidelberg, New York, pp. 39–46.

Nézan, E., Tillmann, U., Bilien, G. *et al.* 2012. Taxonomic revision of the dinoflagellate *Amphidoma caudata*: transfer to the genus

Azadinium (Dinophyceae) and proposal of two varieties, based on morphological and molecular phylogenetic analyses. *J. Phycol.* **48**: 925–39.

Pascual, M. S. and Zampatti, E. 1999. El cultivo de moluscos bivalvos. *In* Boschi, E. E. (Ed.) *Los Recursos Pesqueros del Mar Argentino*. INIDEP, Mar del Plata, pp. 167–93.

Percopo, I., Siano, R., Rossi, R., Soprano, V., Sarno, D. and Zingone, A. 2013. A new potentially toxic *Azadinium* species (Dinophyceae) from the Mediterranean Sea, *A. dexteroporum* sp. nov. *J. Phycol.* **49**: 950–66.

Potvin, E., Jeong, H. J., Kang, N. S. T., Tillmann, U. and Krock, B. 2012. First report of the photosynthetic dinoflagellate genus *Azadinium* in the Pacific Ocean: morphology and molecular characterization of *Azadinium* cf. *poporum*. *J. Eukaryot. Microbiol.* **59**: 145–56.

Rehmann, N., Hess, P. and Quilliam, M. A. 2008. Discovery of new analogs of the marine biotoxin azaspiracid in blue mussels *Mytilus edulis* by ultra-performance liquid chromatrography/tandem mass spectrometry. *Rapid Commun. Mass Spectrom.* **22**: 549–8.

Salas, R., Tillmann, U., John, U. *et al.* 2011. The role of *Azadinium spinosum* (Dinophyceae) in the production of Azaspiracid Shellfish Poisoning in mussels. *Harmful Algae* **10**: 774–83.

Salas, R., Tillmann, U. and Kavanagh, S. 2014. Morphology and molecular characterization of the small armoured dinoflagellate *Heterocapsa minima* (Peridiniales, Dinophyceae). *Eur. J. Phycol.* **49**: 413–28.

Satake, M., Ofuji, K., James, K., Furey, A. and Yasumoto, T. 1998. New toxic events caused by Irish mussels. *In* Reguera, B., Blanco, J., Fernandez, M. L. and Wyatt, T. (Eds.) *Harmful Algae*. Xunta de Galicia and International Oceanographic Commission of UNESCO, Santiago de Compostela, pp. 468–9.

Smith, K. F., Rhodes, L., Harwood, D. T. *et al.* 2016. Detection of *Azadinium poporum* in New Zealand: the use of molecular tools to assist with species isolations. *J. Appl. Phycol.* **28**: 1125–32.

Sournia, A. 1984. Classification at nomenclature de divers dinoflagellates marines (classe des Dinophyceae). *Phycologia* **23**: 345–55.

Takano, Y. and Horiguchi, T. 2005. Acquiring scanning electron microscopical, light microscopical and multiple gene sequence data from a single dinoflagellate cell. *J. Phycol.* **42**: 251–6.

Taleb, H., Vale, P., Amanhir, R., Benhadouch, A., Sagou, R. and Chafik, A. 2006. First detection of azaspiracids in mussels in north West Africa. *J. Shellfish Res.* **25**: 1067–70.

Tillmann, U., Borel, M., Barrera, F. *et al.* 2016. *Azadinium poporum* (Dinophyceae) from the South Atlantic off the Argentinean coast produce AZA-2. *Harmful Algae* **51**: 40–55.

Tillmann, U., Elbrächter, M., John, U. and Krock, B. 2011. A new non-toxic species in the dinoflagellate genus *Azadinium*: *A. poporum* sp. nov. *Eur. J. Phycol.* **46**: 74–87.

Tillmann, U., Elbrächter, M., John, U., Krock, B. and Cembella, A. 2010. *Azadinium obesum* (Dinophyceae), a new nontoxic species in the genus that can produce azaspiracid toxins. *Phycologia* **49**: 169–82.

Tillmann, U., Elbrächter, M., Krock, B., John, U. and Cembella, A. 2009. *Azadinium spinosum* gen. et sp. nov. (Dinophyceae) identified as a primary producer of azaspiracid toxins. *Eur. J. Phycol.* **44**: 63–79.

Tillmann, U., Gottschling, M., Nézan, E. and Krock, B. 2015. First record of *Azadinium dexteroporum* and *Amphidoma languida* (Amphidomataceae, Dinophyceae) from the Irminger Sea off Iceland. *Mar. Biodivers. Rec.* **8**: 1–1.

Tillmann, U., Gottschling, M., Nézan, E., Krock, B. and Bilien, G. 2014a. Morphological and molecular characterization of three new *Azadinium* species (Amphidomataceae, Dinophyceae) from the Irminger Sea. *Protist* **165**: 417–4.

Tillmann, U., Krock, B. and Taylor, B. 2014b. *Azadinium caudatum* var. *margalefii*, a poorly known member of the toxigenic genus *Azadinium* (Dinophyceae). *Mar. Biol. Res.* **10**: 941–56.

Tillmann, U., Salas, R., Jauffrais, T., Hess, P. and Silke, J. 2014c. AZA: the producing organisms – biology and trophic transfer. *In* Botana, L. M. (Ed.) *Seafood and Freshwater Toxins*. CRC Press, Boca Raton, FL, pp. 773–98.

Tillmann, U., Salas, R., Gottschling, M., Krock, B., O'Driscoll, D. and Elbrächter, M. 2012a. *Amphidoma languida* sp. nov. (Dinophyceae) reveals a close relationship between *Amphidoma* and *Azadinium*. *Protist* **163**: 701–19.

Tillmann, U., Söhner, S., Nézan, E. and Krock, B. 2012b. First record of *Azadinium* from the Shetland Islands including the description of *A. polongum* sp. nov. *Harmful Algae* **20**: 142–55.

Toebe, K., Joshi, A. R., Messtorff, P., Tillmann, U., Cembella, A. and John, U. 2013. Molecular discrimination of taxa within the dinoflagellate genus *Azadinium*, the source of azaspiracid toxins. *J. Plankton Res.* **35**: 225–30.

Torgersen, T., Bruun Bremmens, N., Rundberget, T. and Aune, T. 2008. Structural confirmation and occurrence of azaspiracids in Scandinavian brown crabs (*Cancer pagurus*). *Toxicon* **51**: 93–101.

Trainer, V. L., Moore, L., Bill, B. D. *et al.* 2013. Diarrhetic shellfish toxins and other lipophilic toxins of human health concern in Washington state. *Mar. Drugs* **11**: 1815–35.

Turner, A. D. and Goya, A. B. 2015. Occurrence and profiles of lipophilic toxins in shellfish harvested from Argentina. *Toxicon* **102**: 32–42.

Twiner, M. J., Doucette, G. J., Rasky, A., Huang, X. P., Roth, B. L. and Sanguinetti, M. C. 2012. Marine algal toxin azaspiracid is an open-state blocker of hERG potassium channels. *Chem. Res. Toxicol.* **25**: 1975–84.

Twiner, M., Hess, P. and Doucette, G. J. 2014. Azaspiracids: toxicology, pharmacology, and risk assessment. *In* Botana, L. M. (Ed.) *Seafood and Freshwater Toxins*. CRC Press, Boca Raton, FL, pp. 823–55.

Twiner, M. J., Rehmann, N., Hess, P. and Doucette, G. J. 2008. Azaspiracid shellfish poisoning: a review on the chemistry, ecology, and toxicology with emphasis on human health impacts. *Mar. Drugs* **6**: 39–72.

Ueoka, R., Ito, A., Izumikawa, M. *et al.* 2009. Isolation of azaspiracid-2 from a marine sponge *Echinoclathria* sp. as a potent cytotoxin. *Toxicon* **53**: 680–4.

Vale, P., Bire, R. and Hess, P. 2008. Confirmation by LC–MS/MS of azaspiracids in shellfish from the Portuguese north-west coast. *Toxicon* **51**: 1449–56.

Yao, J., Tan, Z., Zhou, D., Guo, M., Xing, L. and Yang, S. 2010. Determination of azaspiracid-1 in shellfishes by liquid chromatography with tandem mass spectrometry. *Chin. J. Chromatogr.* **28**: 363–7.

SUPPORTING INFORMATION

Additional Supporting Information may be found in the online version of this article at the publisher's web-site:

Fig. S1. Examples of micrographs used to assign plate overlap pattern in *Azadinium luciferelloides*.

Fig. S2. Examples of variability in shape of plates 3′ and 2a, and of deviating plate pattern in *Az. luciferelloides*.

Fig. S3. Quantification of thecal pores in *Az. luciferelloides*.